TRANSIENT SURGE MEASUREMENTS OF A CENTRIFUGAL COMPRESSOR STATION DURING EMERGENCY SHUTDOWNS

by

J. Jeffrey Moore

Program Manager

Augusto Garcia-Hernandez

Research Engineer

Matthew Blieske

Engineer

Southwest Research Institute

San Antonio, Texas

Rainer Kurz

Manager of Systems Analysis and Field Testing

Solar Turbines, Inc.

San Diego, California

and

Klaus Brun

Manager

Southwest Research Institute

San Antonio, Texas

Jeffrey Moore is a Program Manager at Southwest Research Institute, in San Antonio, Texas. His professional experience over the last 18 years includes engineering and management responsibilities related to centrifugal compressors and gas turbines at Solar Turbines Inc. in San Diego, California, Dresser-Rand in Olean, New York, and Southwest Research Institute in San Antonio, Texas. Dr. Moore's interests include advanced compression methods, rotordynamics, seals and bearings, computational fluid dynamics, finite element analysis, controls, and aerodynamics. He has authored more than 20 technical papers related to turbomachinery and has given numerous tutorials and lectures. He is currently the vice-chair of the Oil and Gas Committee for IGTI Turbo Expo.

Dr. Moore holds B.S., M.S., and Ph.D. degrees (Mechanical Engineering) from Texas A&M University.

Augusto Garcia-Hernandez is a Research Engineer at Southwest Research Institute, in San Antonio, Texas. His professional experiences include various experimental works, sales, technical support, drilling research assistant, and drilling laboratory teaching assistant. His Master's thesis focused on cuttings transport velocity in horizontal and highly-inclined wells. In addition to his graduate work, he has been involved in research on double-piston pumps (experimental characterization and evaluation) and progressive cavity pumps (modeling development), as well as drilling fluids applications. Mr. Garcia has publications in areas such as cuttings transport in horizontal and deviated wells, gas pipeline transport, and centrifugal compressors surge analysis.

Mr. Garcia holds a B.S. degree (Mechanical Engineering) from Central University of Venezuela and an M.S. degree (Petroleum Engineering) from the University of Tulsa.

Matthew Blieske is an Engineer with Southwest Research Institute, in San Antonio, Texas. Examples of functions he performs are: troubleshooting turbomachinery in the field, fundamental compressor research, oil and gas facility simulation and design, design and testing of renewable energy technologies, and CO2 compression technology development. Previous work experience includes aerospace gas turbine repair design and overhaul, gas turbine test cell operation, and airline heavy maintenance engineering. Mr. Blieske has published papers on design and simulation of advanced energy systems and compressor transient behavior.

Mr. Blieske has a Masters degree (Mechanical Engineering) from Carleton University in Ottawa, Canada. He started working for SwRI in 2008.

Rainer Kurz is Manager of Systems Analysis and Field Testing for Solar Turbines Incorporated, in San Diego, California. His organization is responsible for conducting application studies, gas compressor and gas turbine performance predictions, and site performance testing. He joined Solar Turbines Incorporated in 1993 and has authored more than 70 publications in the field of turbomachinery.

Dr. Kurz attended the University of the German Armed Forces, in Hamburg, where he received the degree of a Dipl.-Ing., and, in 1991, the degree of a Dr.-Ing. He was elected as an ASME Fellow in 2003 and is a member of the Turbomachinery Symposium Advisory Committee.

Klaus Brun currently manages the Rotating Machinery and Measurement Technology Section at Southwest Research Institute, in San Antonio, Texas. His research interests are in the areas of turbomachinery aerothermal fluid dynamics, process system analysis, energy management, advanced thermodynamic cycles, instrumentation and measurement, and combustion technology. He is widely experienced in performance prediction, off-design function, degradation, uncertainty diagnostics, and root cause failure analysis of gas turbines, combined cycle plants, centrifugal compressors, steam turbines, and pumps. He has been involved in research on automotive torque converters, rotating compressible flows, bearing design, labyrinth seals, instrumentation and data acquisition, laser velocimetry, flow interferometry, complex geometry convection flows, advanced gas turbine cycles, and air emissions technology.

Dr. Brun received his Ph.D. and M.S. degrees (Mechanical and Aerospace Engineering, 1996, 1993) from the University of Virginia, and a B.S.E. degree (Aerospace Engineering, 1991) from the University of Florida.

ABSTRACT

For every centrifugal compressor installation, the design of the surge control system is vitally important to prevent damage of the compressor internal components, seals, and bearings. While most surge control systems are capable of preventing surge for steady-state operation, emergency shutdowns (ESDs) are particularly challenging, since the surge control system must respond faster than the deceleration rate of the train. The available experimental data are not of sufficient quality and resolution to properly validate current software packages. This paper outlines an experimental test program using a full-scale compressor tested in a hydrocarbon flow loop under controlled, laboratory conditions. Transient compressor surge data during an ESD were captured over a variety of initial speed, pressure, and flow conditions. Furthermore, the anti-surge valve was modified in subsequent tests to simulate a slower and a smaller valve, providing a more varied test condition. Results of the testing and model comparisons will be presented.

INTRODUCTION

Currently, computational models are very common and useful for providing quick, reliable, and cost-effective solutions to real problems. In general, pipeline models include a lot of detailed and specific information of the real system being modeled. Therefore, it is important that these data be accurate in order to ensure the predictive capability of the computational model. However, computational simulations have some level of uncertainty and inaccuracy due to the use of simplifications, assumptions, and numeric calculations. Therefore, model developers have to adjust, refine, and validate their models to simulate more accurately the real process and events. Models are validated by comparing the simulation results to known steady-state and transient parameters at various other operating points. However, sometimes this is not an easy task, since poor or no data are available for the tuning process.

The transient behavior of compressor stations, particularly under rapidly changing conditions, is of vital interest to compressor station operators. Predicting transient behavior is an important factor in avoiding damage during events such as emergency shutdowns. A limited number of "accidental" data sets from compressor manufacturers and users are available in the public literature domain. A variety of simulations and modeling approaches has been presented over the last few years at industry conferences.

The available experimental data for transient shutdowns are not of sufficient quality and resolution to compare predictions properly with analytical results or simulations available from current software packages. Necessary information about the compressor, the driver, the valves, and the geometry of the system is often missing. Currently utilized software has not been adequately validated with full-scale realistic benchmark data, as these data are not available in the public domain. Modeling procedures and results of surge control system simulations seldom contain validation data achieved through actual testing. These type of transient test data for a dynamic surge condition are often difficult to obtain.

The possible operating points of a centrifugal gas compressor, operated at variable speeds, are shown in the head-flow characteristic in Figure 1. The operating range is limited by maximum and minimum operating speed, maximum available power, choke flow, and stability (surge) limit. At flows lower than the stability point, the compressor initially shows a reduced capacity to generate head with reduced flow, until it experiences reverse flow; that is, the gas flows from the discharge to the suction side. Once flow reversal occurs, the amount of flow depends on the pressure ratio across the compressor, since, in this situation, the compressor acts more or less like an orifice. The flow reversal means that the pressure downstream of the compressor is gradually reduced. The speed of pressure reduction depends largely on the size of the volume downstream of the compressor. Once the pressure is reduced sufficiently, the compressor will recover and flow gas again from the suction to the discharge side. Unless action is taken, the events will repeat again. Ongoing surge can damage thrust bearings (due to the massive change of thrust loads), seals, and eventually, overheat the compressor. Details of the energy transfer from the compressor into the gas are described in Ribi and Gyarmathy (1997).

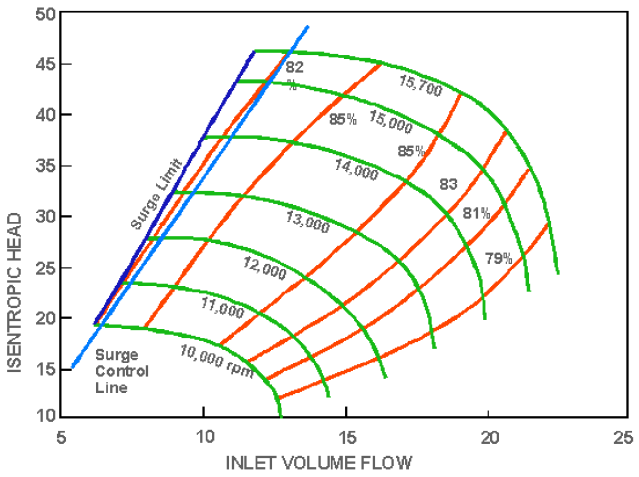

Figure 1. Typical Map of a Variable-Speed Centrifugal Compressor.

Surge has to be avoided to protect the compressor. The usual method for surge avoidance ("anti-surge-control") consists of one or several recycle loops that can be activated by fast-acting valves ("anti-surge valves") when the control system detects that the compressor approaches its surge limit. Typical control systems use suction and discharge pressure and temperature together with the inlet flow into the compressor as input to calculate the relative distance ("surge margin") of the present operating point to the predicted or measured surge line of the compressor (Figure 1). The surge margin (SM) is defined by:

$$SM = \frac{Q_{op} - Q_{surge}}{Q_{op}} \Big|_{N=const} \quad (1)$$

It should be mentioned that the definition of the surge line is somewhat arbitrary, especially because it is ultimately a system feature, not an isolated compressor feature. Definitions frequently used to establish this line include a local maximum in the head-flow characteristic, the onset of rotating stall (usually established from vibration signatures or by the use of theoretical criteria), the onset of high vibrations (either broadband or at distinct frequencies), or the point where actual flow reversal is established.

If the surge margin reaches a preset value (often 10 percent), the anti-surge valve starts to open, thereby reducing the pressure ratio of the compressor and increasing the flow through the compressor.

The anti-surge control system has to cover different tasks (Brun and Nored, 2007; White and Kurz, 2006):

- Facilitate the starting and normal shutdown process.
- Accommodate slow process changes to prevent process disruption. Precisely positioned valves ensure that no oscillations occur.
- Accommodate fast process changes and massive system disturbances (for example, during emergency shutdowns). This requires fast system reaction and, among other things, extremely fast-opening valves with sufficiently large flow areas.

Emergency shutdowns (ESDs) tax the reaction of the entire system. Here, the fuel supply to the gas turbine driver is cut off instantly (some installations maintain fuel flow to the turbine for 1 to 2 seconds while the recycle valve opens; however, this can generate a safety hazard). In electric, motor-driven installations, the ESD is initiated by tripping the motor. In either case, the compressor train will decelerate rapidly under the influence of the fluid forces counteracted by the inertia of the rotor system. Because the head-making capability of the compressor is reduced by the square of its running speed, while the pressure ratio across the machine is imposed by the upstream and downstream piping system, the compressor would surge if the surge valve could not provide fast relief of the discharge pressure. A 30 percent loss in speed, which is very common in ESD scenarios, equates to a loss in head of approximately 50 percent (Kurz and White, 2004). The valve must therefore reduce the pressure across the compressor by about half, in the same time as the compressor loses 30 percent of its speed.

The rate at which the discharge pressure can be relieved not only depends on the reaction time of the valve, but also on the time constraints imposed by the piping system. The transient behavior of the piping system depends largely on the volumes of gas enclosed by the various components of the piping system, which may include, besides the piping itself, various scrubbers, knockout drums, and coolers (Figure 2).

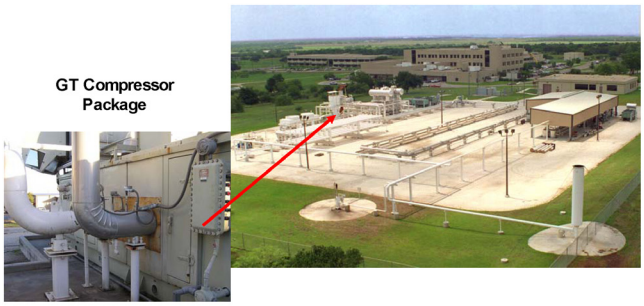

Figure 2. Views of Meter Research Facility and Centrifugal Compressor and Turbine.

The larger the volumes are in the system, the longer it will take to equalize the pressures. Obviously, the larger the valve, the better the potential of the system to avoid surge. However, the larger the valve, the poorer its controllability at partial recycle and the slower the opening time. The faster the valve can be opened, the more flow can pass through it, especially in the first few critical seconds following an ESD. There are, however, limits to the valve opening speed dictated by the need to control intermediate positions of the valve as well as by practical limits to the power of the actuator. The situation may be improved by using a valve that is only boosted to open, thus, combining high opening speed for surge avoidance with the capability to avoid oscillations by slow closing. If the discharge volume is too large and the recycle valve cannot be designed to avoid surge, a short recycle loop (hot recycle valve) may be considered, where the recycle loop does not include the after-cooler.

Other authors have successfully developed transient surge models that predict the behavior of the compression systems during an ESD (Morini, et al., 2007; Botros and Ganesan, 2008). However, correlations are made to laboratory-scale compression systems. The current paper presents results and predictions for a full-scale natural gas centrifugal compressor that is fully instrumented to provide both accuracy and realism.

The primary objective of this work was to develop experimental transient compressor surge data during shutdowns, which would facilitate the verification and comparison of existing and future transient surge models. Results of the testing and model comparisons are documented. Relevant, dimensionless parameters are presented and validated utilizing the test data. Conclusions from the testing and recommendations for the transient analysis software are provided. High-resolution and high-fidelity compressor surge and piping system transient data were measured from full-scale experiments. These data were utilized for benchmarking existing transient flow solvers that are currently employed by the industry to design compressor station surge control systems. Fluid transients and compressor performance of the onset of surge or full surge are documented for 20 different pressure/flow conditions. In addition, another four different nonsurge fluid transient events were tested. The system transient tests were induced by ESD events. The test conditions were as representative as possible of actual compressor surge events and both the onset as well as full surge events are documented.

The surge data generated during the testing at the lead author's company's meter research facility (MRF) includes all deceleration lines of the centrifugal compressor during the shutdown. In addition, all transient sequences, including traveling time of the valves and compressor ramp-down curve, have been recorded. Performance test data of the centrifugal compressor were also collected. Dynamic modeling of the compressor and the entire loop was conducted using transient flow simulation software. Therefore, a wide set of conditions were available for modeling validation, tuning, and performance predictions.

EXPERIMENTAL SETUP

The surge testing was performed at the MRF. The MRF is a meter calibration research facility located in San Antonio, Texas. It comprises two closed-loop natural gas flow facilities, the high pressure loop (HPL) and lower pressure loop (LPL). The surge testing was performed on the HPL, which has a centrifugal compressor driven by a 1300 hp gas turbine. The HPL operates at line pressures from 150 to 1100 psig and flow rates up to 1380 ACFM. The test gas was processed natural gas supplied by the city energy utility. A gas chromatograph with dual columns was used to determine the gas composition via analysis up to C_{9+}. A bank of critical flow Venturi nozzles (sonic nozzles) were the basis for determining the reference flow rates. Several temperature and pressure transducers were installed in the facility for gas temperature and pressure determination. Figure 2 shows views of the HPL and LPL, with a close-up view of the gas turbine and centrifugal compressor.

For comparison purpose, the inertia number as defined by Botros and Ganesan (2008) is shown in Table 1. The value for the MRF falls between 30 and 100, where a detailed simulation is recommended.

Table 1. Summary of Inertia Number Established by Botros and Ganesan (2008) for the MRF Compressor Facility.

Botros and Ganesan Inertia Number						
DATA POINT	Speed [RPM]	Inertia [Kg.m^2]	Mass Rate at Surge [kg/s]	Head at Surge [J/kg]	Delay Time [s]	Inertia Number N_{BG}
MRF#1	17800	0.19	4.49	16487.1	0.18	50
MRF#2	19800	0.19	4.78	20532.8	0.18	47

Several standard pieces of equipment exist in the MRF that were used for the operation of the test loop. Figure 3 shows a picture of the recycle valve. Other equipment includes the suction and discharge valves, suction and discharge piping, discharge cooler, and suction scrubber. All of this equipment was utilized during the surge testing.

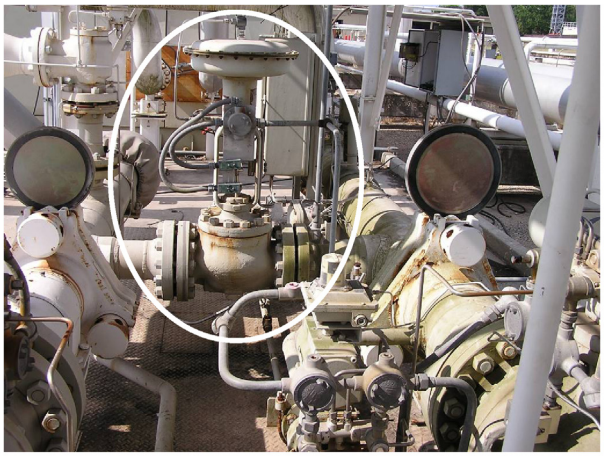

Figure 3. View of Recycle Valve and Suction and Discharge Piping at MRF.

In order to collect high-resolution and high-fidelity data for a compressor surge event, high-frequency-response and accurate instrumentation were utilized. The surge testing setup was defined to measure the most important variables of a normal compressor system, such as suction and discharge pressures and temperatures, compressor speed and vibrations, gas flow rate, etc., while including the key parameters of the anti-surge control system. Parameters such as recycle valve travel, timing, and differential pressure, suction and discharge valve travel time, and differential pressure were monitored and recorded to capture the existing anti-surge control sequences.

This setup allowed for transient tests intended to collect high-fidelity transient data of full-scale emergency shutdowns (ESD, fast stop) of a centrifugal compressor under different initial operating conditions. The transient data included static and dynamic line pressure (absolute and differential) from different locations, compressor speed, suction and discharge temperatures, and machine vibration data. The absolute pressure transducers were mounted close to the piping and had a response bandwidth (2000 Hz) capable of measuring both the mean (direct current, DC) and fluctuating (alternating current, AC) pressure components. Data acquisition included use of a 24-bit A/D high-frequency data recorder with 16 channels of parallel sampling. In addition, performance tests were conducted to determine the existing status of the unit and to obtain its performance curves. The installation diagram identifies the suction and discharge valves, the recycle valve, the discharge cooler, and the suction scrubber. The test setup included valves on the suction and discharge sides of the compressor. These valves were automatically closed at the initiation of a shutdown and travel from fully open to fully closed required two seconds.

Although the entire high pressure loop of the MRF was utilized for these tests, the principal component monitored was the centrifugal compressor. This compressor was a single-stage centrifugal compressor with a 7½ inch diameter impeller. The compressor driver's ISO power output is 1560 hp. It was directly connected to the centrifugal compressor. The compressor setup included suction and discharge headers, a gas scrubber, after-cooler, isolation valves, vibration monitoring system, and recycle valve.

The suction header was a 12 inch diameter (schedule 80) pipe that connected to an isolating suction valve and then to a 31 × 115 inch scrubber to finally reach the suction side of the centrifugal compressor. Along its path, the suction header had several taps that were utilized to mount the test instrumentation. From the compressor discharge, an 8 inch diameter pipe connected to a fin-fan after-cooler. Downstream of this cooler was a recycle loop and then a discharge isolation valve. The recycle loop was a small segment of pipe that connected the suction with the discharge header through a control valve. The control valve was part of the surge control system of the machine. This surge control system monitored various parameters, such as suction and discharge pressure and flow rate, to control the recycle valve position. All the surge control was accomplished through pneumatic programmable relays. The recycle control valve (REV) was a 6 inch diameter, equal-percentage (Cv_{max} = 394 gpm/psi^{½}), quick-opening valve that was actuated pneumatically. Its normal position was open. This allowed the possibility of controlling the opening time by adding a valve in the vent of the actuator diaphragm. A general schematic of the compressor setup is presented in Figure 4 including the locations of the instrumentation used.

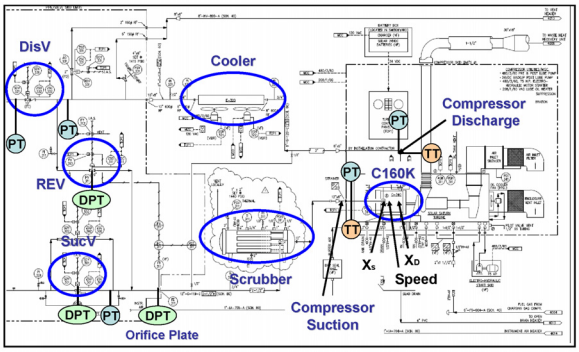

Figure 4. General Schematic of the Centrifugal Compressor at MRF.

INSTRUMENTATION

High-accuracy and high-frequency-response instrumentation was used for measuring all the variables involved in the surge testing. A total of 16 different signals was monitored and recorded. Pressure measurements were taken using high-accuracy (0.1 to 0.25 percent) line pressure and differential pressure transducers that had a frequency-response bandwidth of 2000 Hz. A 12-24 DC excitation voltage powered these transducers, while the output was DC-coupled. Gas temperature was measured using two thermocouples located at the compressor suction and discharge. Radial shaft vibration data on the compressor were collected from the vibration monitoring system located in the external control panel of the compressor. In addition, two more vibration signals were obtained from vibration probes installed in the unit, resulting in X-Y data on both ends. Compressor speed was measured through a magnetic pick-up sensor located on the shaft of the power turbine of the driver. The frequency signal was converted to a voltage signal by using a frequency-to-voltage converter. A linear variable differential transformer (LVDT) was used for measuring linear displacement of the recycle valve, allowing stroke length and travel time of the recycle valve to be measured. In addition, all the instrumentation was calibrated and verified prior to its installation in the MRF for both testing phases. Figure 5 shows some of the instrumentation connected at the compressor side of the MRF.

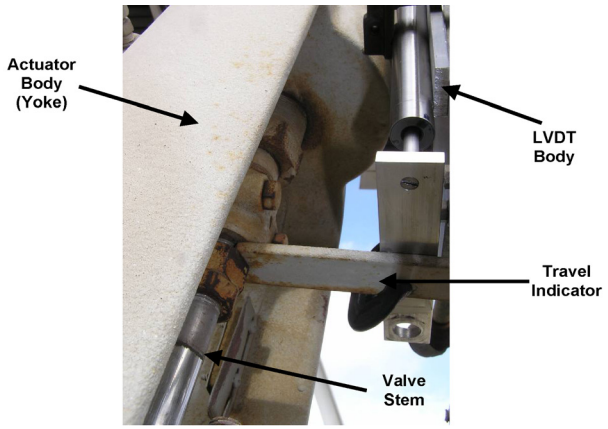

Figure 5. Recycle Valve Actuator with the LDVT Connection.

MODIFICATIONS

The centrifugal compressor has a surge control system installed, which was designed to avoid surge and operate the compressor along the operating surge line. The surge control system had to be modified to allow the compressor to reach the measured surge line during testing. The recycle valve on the control system was integral for controlling whether the compressor surged or not. Changing the operation of this valve allowed the compressor to be operated closer to the measured surge line. The recycle valve in the surge control system was a globe valve with a pneumatic actuator that opened and closed the valves with two inches of travel. Two parameters could be controlled on the valve for surge control: the rate at which the valve opened and closed and the distance the valve traveled.

Changing the rate at which the valve traveled changed the response of the surge control system. Usually, recycle valves are set to open as quickly as possible. This allows recycle flow to begin quickly, increasing the flow in the compressor and, thereby, moving the compressor from the surge line quickly. If the rate the valve opens is decreased, recycle flow will start later, resulting in compressor operation closer to the surge line. The rate at which the recycle valve opened and closed was controlled by installing a needle valve on the vent of the actuator diaphragm as shown in Figure 6. This allowed a backpressure (higher than atmospheric pressure) to be applied to the diaphragm, which slowed the rate at which the valve opened or closed. The needle valve had increments labeled on its adjusting knob as shown in Figure 6. This allowed various valve opening rates to be tested repeatedly with accuracy.

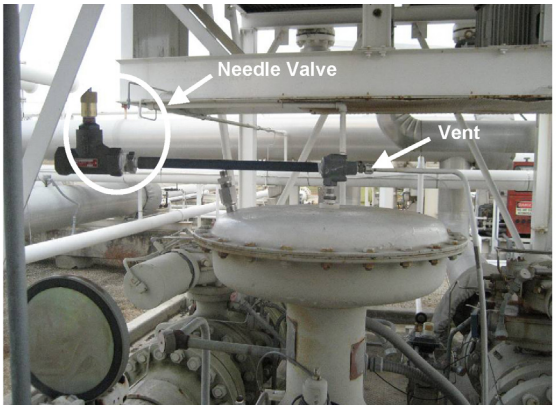

Figure 6. Recycle Valve Actuator Diaphragm with a Needle Valve in the Vent.

The surge control system was modified by also varying the distance the valve stem traveled during opening of the recycle valve. Varying this distance simulated what the operation of the recycle valve would be for different valve sizes. For example, limiting the valve travel simulated a smaller recycle valve, which would allow less recycle flow. This allowed the compressor to operate closer to the surge line during the ESD. The recycle valve had a two inch travel end-to-end. Clamps were placed on the valve stem to act as mechanical stops. These restricted the opening of the valve to various positions.

DATA ACQUISITION

For acquiring the test data, a 16-channel analyzer system was used. This system collected steady-state and transient data with a 24-bit data acquisition, accepting voltage input signals in the range of ±20 Volts. The data acquisition system was installed at the testing site (near the compressor) and a fiberoptic network was run from the system to the control room where operation of the compressor was controlled. Signals from all instrumentation were acquired with this system. The graphs observed through the data acquisition system show several measurement readings taken during a shutdown/surge of the compressor: compressor suction and discharge pressure, compressor speed, seat position of the recycle valve, pressures across the suction and discharge valves, and vibration data from the compressor. The data recorded by the data acquisition system were exported to a spreadsheet for processing after each test was completed.

EXPERIMENTAL TEST PROCEDURE

Several pre-test activities were required for both the steady-state and transient tests. These included checking the control panels, checking valve line-ups, starting the glycol, hot oil, and chiller pumps, starting the reciprocating compressor that provides fuel gas to the gas turbine that powered the test compressor, and opening the 4 inch bypass valve. Once these activities were completed, the gas turbine was started. The gas turbine unit was run at its idle speed for two to three minutes or the automatic startup sequence was initiated. The gas turbine slowly built up speed as it approached the steady-state initial condition required. During this process, the bypass valve closed or opened based on the required flow conditions for the compressor. Once the gas turbine reached full speed, the system was allowed to stabilize at the desired operating condition. At the MRF, there were several flow control nozzles used to regulate and measure the flow through the test loop. Once the gas turbine stabilized, the appropriate nozzles were opened to obtain the required flow condition.

Next, either a performance test or surge test was performed. For both types of tests, the compressor was first set at the desired compressor speed and flow. The flow was reduced by partially closing the bypass valve. The system was allowed to stabilize for 15 minutes. After stable conditions had been achieved, the test data were recorded. If a performance test was conducted, then the test was ended. Then either another performance test point was taken or compressor shutdown was engaged and post-test activities were completed.

For surge testing, the data acquisition system began recording the transient data (first-in, first-out [FIFO] data) from steady-state initial conditions. Once the data acquisition began, the shutdown sequence of the compressor was started (fast stop sequence). After the compressor had come to a complete stop, the data acquisition system was stopped and the test data were saved. Once a compressor shutdown was completed and the transient data were saved, the unit was restarted if another test needed to be completed. After all testing was complete, the gas turbine and reciprocating compressor were shut down. In addition, the glycol, hot oil, and chiller pumps were shut down.

The surge testing was conducted in two phases. The first phase focused on defining the testing methodology, designing the instrumentation and data acquisition system, and testing surge at low suction pressure. After the first phase of surge testing, enough experience was gained to proceed to testing high-suction-pressure surge. In Table 2 and Table 3 are the test matrices for the first and second phase of testing.

Table of Contents

Table 2. Surge Testing Phase I—Test Matrix.

INITIAL POINT DATA FOR SHUTDOWN SEQUENCES												
Test ID	Comp Suc [psia]	Comp Disch [psia]	Tsuc [°F]	Tdis [°F]	Mass Flow [lbm/s]	Actual Flow (cfm)	Standard Flow [MMSCFD]	Compressor Speed (RPM)	P2/P1	T2/T1	INITIAL SURGE MARGIN [%]	Compressor Isentropic Head [ft]
P1-1	188.3	208.3	70.4	87.8	13.66	1400.8	26.38	17700	1.106	1.249	38.6	4810.0
P1-2	186.2	208.1	70.7	89.3	11.54	1203.2	22.29	17778	1.118	1.263	28.5	5328.6
P1-3	185.1	208.0	71.5	90.7	10.17	1071.6	19.65	17777	1.124	1.268	19.7	5600.7
P1-4	184.6	207.0	72.5	92.2	8.84	938.4	17.08	17850	1.122	1.271	8.4	5519.0
P1-5	185.1	209.2	72.3	93.6	15.52	1618.8	29.98	19800	1.131	1.295	41.0	5903.4
P1-6	182.4	209.3	73.2	96.1	13.12	1399.3	25.34	19879	1.148	1.313	31.7	6650.4
P1-7	180.9	209.3	74.1	98.1	11.45	1237.6	22.11	19878	1.157	1.322	22.8	7044.3
P1-8	180.6	208.3	74.8	99.0	10.12	1100.7	19.56	19878	1.153	1.323	13.2	6920.7
P1-9	181.0	208.6	75.4	99.5	10.13	1101.7	19.58	19801	1.152	1.320	13.3	6884.3
P1-10	180.7	202.6	73.7	93.3	8.66	941.1	16.73	17778	1.121	1.267	8.6	5516.5
P1-11	177.5	204.4	72.6	96.8	9.73	1072.9	18.79	19800	1.152	1.333	11.0	6831.6

Table 3. Surge Testing Phase II—Test Matrix.

INITIAL POINT DATA FOR SHUTDOWN SEQUENCES										
Test ID	Comp Suc [psia]	Comp Disch [psia]	Tsuc [°F]	Actual Flow (cfm)	Standard Flow [MMSCFD]	Compressor Speed (RPM)	P2/P1	Initial Surge Margin [%]	Compressor Isentropic Head [ft]	REV opening time (s)	REV CVO
P2-1	191.7	221.7	71.2	1204.0	23.0	19804	1.156	20.7	6997.3	1.810	394.0
P2-2	195.4	225.8	70.3	1195.6	23.3	19804	1.156	20.1	6942.0	1.930	394.0
P2-3	192.0	222.3	70.6	1194.6	22.9	19805	1.158	20.1	7036.2	7.190	394.0
P2-4	195.1	225.4	70.6	1202.1	23.4	19804	1.155	20.6	6937.1	1.190	223.6
P2-5	201.3	233.0	71.2	1196.9	24.0	19806	1.157	20.2	7002.1	0.984	96.8
P2-6	201.4	233.2	71.1	1199.7	24.1	19806	1.158	20.4	7036.0	1.460	18.8
P2-7	380.2	442.2	67.7	1202.8	47.1	19802	1.163	20.6	7038.3	1.970	394.0
P2-8	380.2	442.1	67.7	1203.2	47.1	19722	1.163	20.6	7040.9	1.970	394.0
P2-9	381.3	443.3	68.8	1197.8	46.9	19722	1.163	20.3	7040.5	6.770	394.0
P2-10	377.0	438.5	68.4	1201.1	46.6	19804	1.163	20.5	7053.8	2.240	394.0
P2-11	378.3	439.5	68.2	1203.7	46.9	19804	1.162	20.7	6999.0	0.965	228.0
P2-12	379.7	440.7	68.2	1204.9	47.1	19805	1.161	20.7	6950.7	1.140	101.2
P2-13	374.9	435.1	68.8	1228.5	46.0	19803	1.161	22.3	7164.3	1.670	17.9

During Phase I testing, low suction pressure surge events were conducted. The tests were started at two target speeds: 17,800 and 19,800 rpm. The discharge pressure of the compressor was low in order to have a low energy surge. The initial surge margin for all the tests varied from 9 to 40 percent. A range of initial surge margins was evaluated at each speed. Flow through the compressor was varied for each speed to obtain different initial surge margins. Phase I tests were considered as baseline tests, providing operational experience prior to performing the high-suction-pressure surge tests in Phase II. Some of the results from this first phase of testing were first published by Moore, et al. (2009). They are reproduced here for completeness.

Phase II tests were high-energy surge events. The objective of these tests was to see the effects of higher-pressure conditions (high-energy surge) and to see the effects of other parameters on surge, such as recycle valve operation. Recycle valve operation was varied by changing the rate at which the recycle valve opened and by varying the size of the valve or flow restriction. Travel time of the recycle valve varied from 100 to 300 percent of normal operation when the valve was fully opened during shutdown (normal operation was 1.81 seconds). The flow restriction or size of the valve was varied from 5 to 100 percent of normal operation. These tests were all started at a target speed of 19,800 rpm. Each test was started with an initial surge margin of 20 percent.

PERFORMANCE

The first set of test data was gathered under steady-state conditions, with the purpose of establishing the steady-state performance of the compressor at different speeds (Figure 7). To exclude potential inaccuracies in manufacturer-supplied compressor data, the compressor was performance-tested. In this particular case, the head-flow characteristics matched the prediction quite well.

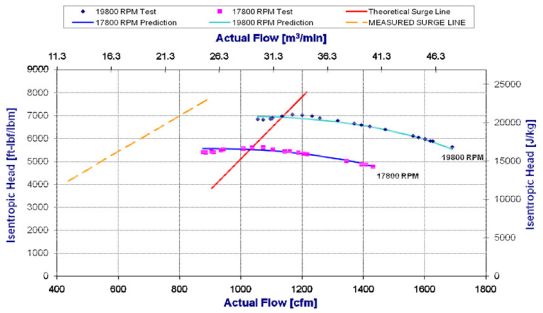

Figure 7. Steady-State Compressor Head-Flow Map for Two Speeds.

With steady-state performance established, two series of tests were performed to determine the transient performance of the system. The test matrices are outlined in Table 2 and Table 3. The first series of tests involved initiating an emergency shutdown at low line pressure with the compressor operating at 17,800 rpm and 19,800 rpm at various surge margins. The second series involved initiating emergency shutdowns at a higher speed (19,800 rpm) and high line pressure with the compressor operating with a 20 percent surge margin when the emergency shutdown was initiated. The results of the surge tests are discussed below.

SURGE TESTING

Phase I Test Results

The first series of tests involved a low-energy surge and two compressor speeds. Figure 8 and Figure 9 show the path (locus) that the compressor followed during each shutdown. The most critical cases occurred when the shutdown was initiated at a low initial surge margin (e.g., P1-11 in the 19,800 rpm case). The trace for P1-11 in the 19,800 rpm case (Figure 9) also has markers for significant system events, such as recycle valve (REV) opening 35.9 percent and fully open. It shows that the compressor actually operated past its stability line with minimum flow being reached at 35.9 percent valve opening. However, due to the system characteristics, no full-flow reversal (surge) occurred. At this point, flow through the recycle valve and associated discharge pressure drop had become large enough to move the compressor operating point back across the surge line into the stable operating region. The minimum flow (600 ACFM) was similar for each speed, but the potential for surge was greater for the higher speed case.

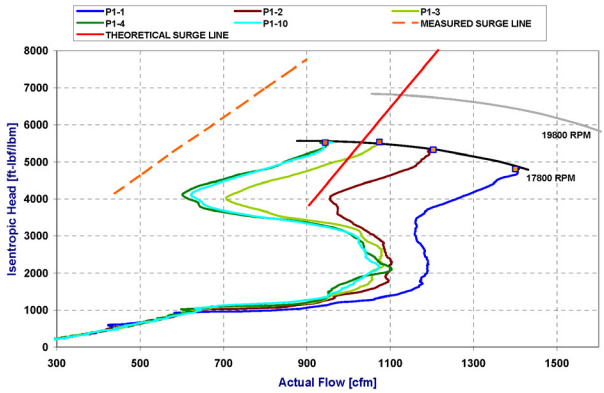

Figure 8. Transient Shutdown Loci Measurements for 17,800 RPM. (Courtesy Moore, et al., 2009)

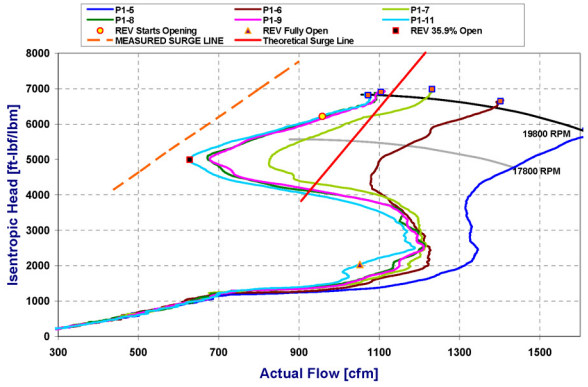

Figure 9. Transient Shutdown Loci Measurements for 19,800 RPM. (Courtesy Moore, et al., 2009)

To appreciate the time sequence of the events, traces for measured process variables in the time domain for each test were

calculated. Discharge pressure rapidly declined after initiation of the shutdown, while suction pressure started to increase toward the settle-out condition. The discharge valve was fully closed (and, thus, built up differential pressure) after about four seconds. These flow conditions did not result in hard surging, as the pressure downstream of the valve also dropped. Data were recorded eight seconds prior to shutdown to determine the initial operating point.

Temperature traces indicated an almost constant discharge temperature during the initial five seconds of the shutdown event. This was mostly due to the thermal mass of the compressor, which kept the discharge temperature from falling with the reduced head the compressor produced as it spun down. The suction temperature reacted much faster to the inflow of hot gas from the compressor discharge.

Head and speed traces showed a rapid reduction of compressor speed and head after the shutdown was initiated. There was a delay of about 200 milliseconds because the gas turbine still produced power even after the fuel was shut off. Shortly after, speed rapidly decreased and the compressor lost about 15 percent of its initial speed in the first second. The minimum flow was reached 1100 milliseconds later, and the corresponding valve opening of 36 percent was identified at that point.

Traces of the differential pressure over the suction and discharge side unit valves indicate a pressure differential near zero for a fully open valve and increases when the valve closes. The test data indicate it took two seconds for the discharge valve to close, and almost three seconds for the suction valve to close. The differential pressure through the discharge valve dropped to a negative value due to a reverse flow from the discharge volume to the suction side through the recycle valve. Although there is a discharge check valve, the data indicate that it was not checking in the first few seconds of the transient event. Therefore, the discharge volume moved backward to the suction side through the recycle valve, since it represented a sink due to its lower pressure condition.

In addition a waterfall plot of the proximity probe located at the discharge of the compressor unit indicates the vibration decay while the unit was coasting down. No evidence of harsh surge was obtained during the transient event. Detailed results from the Phase I tests are outlined in Moore, et al. (2009 and 2009).

Phase II Test Results

A second series of tests was completed to evaluate the effect of varying the recycle valve characteristics while operating with both low and high compressor suction energy. The results are shown in Figure 10 and Figure 11. While the anti-surge system was able to prevent a hard surge event despite altering the recycle valve full-open CV and travel times, recycle flow was not always sufficient to achieve a significant characteristic flow rate increase during shutdown. Tests P2-3, 5, and 6 in Figure 10 illustrate this. Although damaging surge events were not observed during these tests, this behavior suggests that the altered capacity of the recycle valve was marginally sufficient to prevent surging. While no damage to the compressor train was detected, Figure 11 shows Test P2-13 to be a significant surge event.

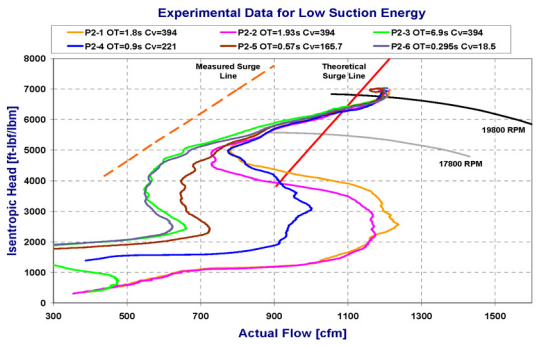

Figure 10. Transient Shutdown Loci for 200 PSIA Suction Pressure Testing.

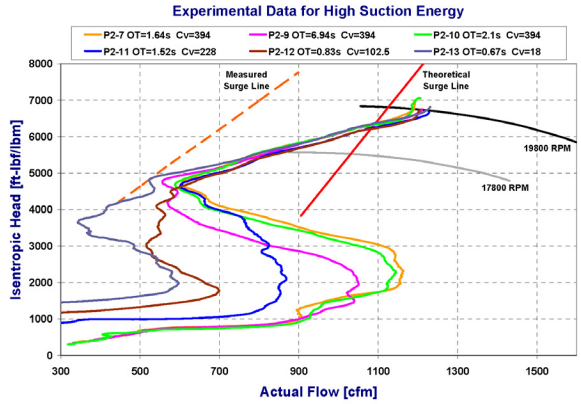

Figure 11. Transient Shutdown Loci for 380 PSIA Suction Pressure Testing.

Figure 12 and Figure 13 are examples of pressure and temperature data at the suction and inlet of the compressor. These results are consistent with the first phase of testing.

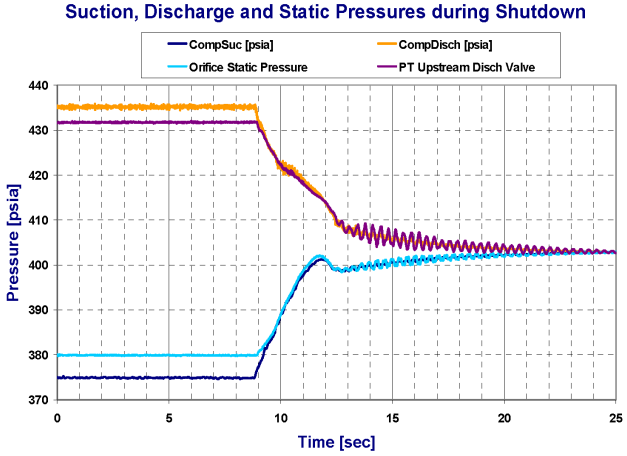

Figure 12. Pressure Data During Shutdown for Test P2-13.

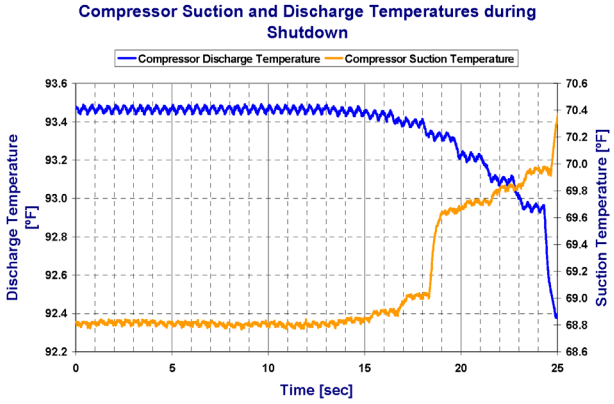

Figure 13. Temperature Data During Shutdown for Test P2-13.

The sequence of events during shutdown is easily identified in Figure 14. Again, the results are similar to Phase I results with different flow and head values. Unlike during the lower suction pressure tests, flow increase typically occurred later than the one-third recycle valve open position previously reported (as seen in Figure 14). The combination of a higher energy inlet flow, reduced recycle valve capacity, and slower valve response time effectively delayed the anti-surge response time.

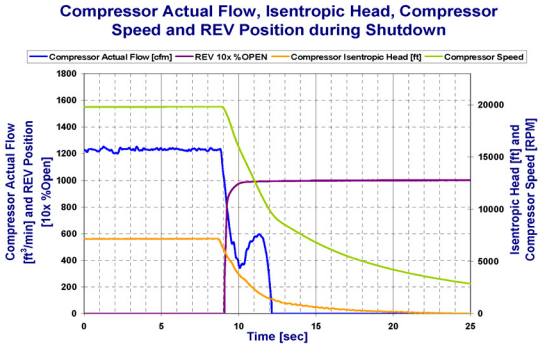

Figure 14. Shutdown Sequence Data for Test P2-13.

Compressor speed (rpm) decay was very similar for both high and low suction pressure tests, shown in Figure 15. Two distinct regions are evident, one quasi-linear region immediately after the shutdown event occurred followed by a shallow parabolic region. Despite varying the inlet pressure (low versus high suction pressure), the total head rise across the compressor was similar for all test cases. As compressor rpm did not vary significantly (less than 80 rpm), system shutdown occurred while the compressor was operating at the same point on the compressor map for all test cases. Hence, similar decay curves in Figure 15 were expected for all cases of Phase II testing. Due to low deviation in rpm decay data for Phase II measured tests, an average decay curve was derived for use in the simulation. This will provide a comparison to the decay curve calculated from theory, which is discussed later.

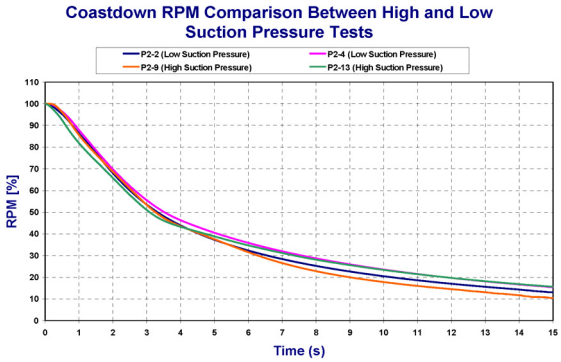

Figure 15. Measured RPM Decay Comparison Between High and Low Suction Pressure Tests.

During Phase I testing, a negative pressure differential was observed across the discharge valve. This behavior was repeated in Phase II for both high and low suction pressure tests, shown in Figure 16. While the discharge pressure differential did not drop to negative values, a noticeable drop was demonstrated before the check valve engaged. Once engaged, the differential pressure rose briefly before flow through the recycle valve was significant enough to reverse flow through the discharge valve.

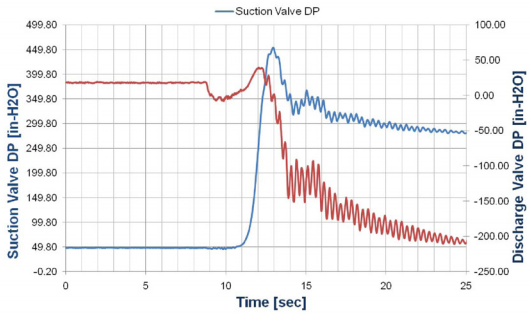

Figure 16. Suction and Discharge Valve Differential Pressure During Shutdown for P2-13.

Figure 17 shows a waterfall plot of the proximity probe located at the discharge of the compressor unit. Vibration decays are observed in these plots while the unit was coasting down. A synchronous vibration of 0.884 mils peak-to-peak was observed during the steady-state condition in the probe located at the discharge of the compressor and minor subsynchronous vibrations were observed during the steady and transient condition as well. These subsynchronous vibrations increased up to 0.752 mils peak-to-peak at 40 Hz at the beginning of the ESD indicating momentary surge was encountered. The vibrations then decayed while the unit was coasting down.

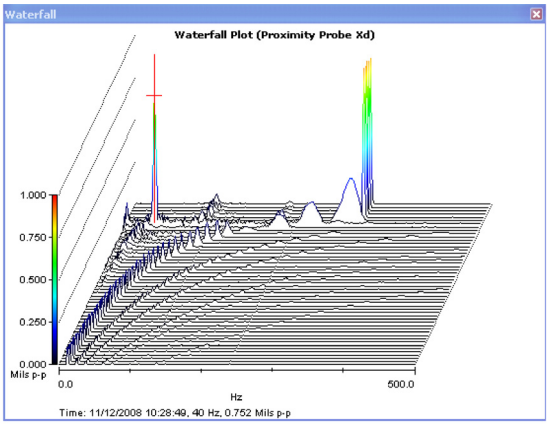

Figure 17. Waterfall Plot of Test P2-13—Xd Proximity Probe.

ANALYSIS OF RESULTS

An interesting result was found in the rpm decay for both high and low suction pressure tests. Figure 18 shows very similar curves, irrespective of suction pressure. There were two distinct portions of the coast down demonstrated in all tests: a region of quasi-linear deceleration, followed by a shallow parabola. The transition between the two regions was sharp and coincided with the point at which flow stopped increasing and began a continuous, parabolic decrease to zero. The different deceleration curves are believed to correspond to two different driving phenomena: the quasi-linear region appeared to be dominated by aerodynamic effects of the compressor, whereas the shallow parabolic region was dominated by inertia of the compressor train. With a high head across the compressor and a significant volume of fluid upstream, the compressor blades continued to generate lift after the fuel was shut off. With little power being delivered to the compressor, this lift was a source of braking and energy dissipation. The level of energy dissipation directly corresponded to the energy potential across the compressor. This effect was more significant than simple inertial deceleration; hence, the steep negative slope when compared to the second region of deceleration, which was inertially dominant. As the energy at the suction of the compressor reduced, the deceleration curve became proportional to the square of the rotational speed and spun down as inertia was bled off.

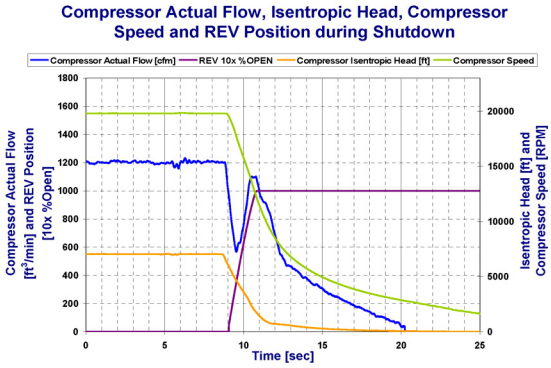

Figure 18. Shutdown Sequence Data for Test 7 (High Suction Pressure, No Recycle Valve Alteration).

Nonlinear actuation behavior was observed for the recycle valve for some test cases, as shown in Figure 14. As this nonlinearity was limited to the last 5 percent of opening, linear actuation was still assumed for modeling purposes. As the recycle valve was a globe style, it is believed that the CV did not change significantly over the last 5 percent of travel.

In both Phase I and Phase II, a delayed discharge check valve response was observed. This allowed flow to recirculate from the high-pressure discharge side to the low-pressure suction side through the gradually opening recycle valve. This further increased the recycled flow delivered to the compressor beyond what the recycle valve would have delivered had the check valve deployment not been delayed. While this did not pose harm to the system, it introduced an error into the simulation, as a delayed check valve was not characterized or modeled.

For Phase II testing, it appears that only Test P2-13 demonstrated surge conditions, shown in Figure 11. This test represented the most severe reduction in surge protection of all Phase II tests, with an equivalent valve size of 1.2 inches having been reduced from six inches (CV at open of 18 compared to 394 with full valve travel). All other tests maintained sufficient flow to maintain some degree of surge margin, as determined from the measured surge line. Test P2-12 was conducted with a full open CV of 102.5, corresponding to an equivalent valve size of 2.5 inches. This test demonstrated very little surge margin at minimum flow, but proved the recycle valve was significantly over-designed for the suction pressure tested. For Phase I testing, P1-7 had a similar surge margin and compressor head when compared to Test P2-12 of Phase II. As was expected, the recycle valve was also over-designed at a lower suction pressure for a similar starting point on the compressor map. As the MRF loop can handle much higher pressures, the surge system was designed for significantly higher suction pressure flows than what was tested.

For testing without recycle valve alteration, minimum flow conditions occurred at about one-third recycle valve opening. This observation was independent of suction pressure since it was observed in the Phase I as well. As recycle valve travel reduction and travel time increase became more severe, this observation was no longer valid. Figure 14 shows the worst case tested (Test P2-13), where the recycle valve was 90 percent open almost a full second before minimum flow was reached. This result was expected, as a higher restriction on recycle flow delayed the minimum flow condition and reduced the minimum surge margin during coast down.

MODELING APPROACH

The objective of this modeling study was to compare experimental results with a computational analysis. This allowed the accuracy of the dynamic model to be evaluated while identifying key points that must be considered to improve the transient analysis. A sensitivity analysis of the relevant parameters was conducted to identify the effect of each in the final predictions.

In the past, transient simulations of centrifugal compressors have been conducted with large, special-purpose computer codes, which required extensive specific input data and considerable computer execution time. The lead author's company has implemented the use of transient flow simulation to model rapid trips of centrifugal compressors, which lead to energetic and potentially damaging surge events. These simulations accounted for the operation of recycle valves, their actuators, vent valves, compressor coast down speed, and control system responses, while including the effects of upstream and downstream piping, scrubbers, after-coolers, parallel compressors, and other features of the compressor installation.

Transient flow simulation (TFS) software solves nonlinear systems of differential equations at each time step using the method of characteristics. Transient analysis consists of a linearized solution of partial differential equations. The optimum time step for the computations is automatically determined by TFS without sacrificing accuracy. Every time step will depend on the transient sequence and event simulated. However, the user could implement his or her own time step for validation of the software accuracy. The time step varies dynamically depending on hydraulic conditions. Very small time steps are required to model transients, but larger time steps are used when the model is relatively steady.

Analysis Process

The quantitative analysis of the system was based on fluid simulation utilizing the TFS software. The process of creating a system model consisted of a review of the available data for the system, creating a functional process block diagram, developing a system model in the TFS software, running the simulation based on initial and boundary operating conditions, validation of the model, and analysis of the resulting simulation data. The computational model allowed for the evaluation and comparison of various operating conditions of the system.

A functional process block diagram was created based on the data collected from the experimental facility used to conduct the tests. Figure 19 shows the functional block diagram (FBD) of the MRF. This phase of the process also included collection of some basic data that were needed in the computational model, such as compressor maps and other operational parameters.

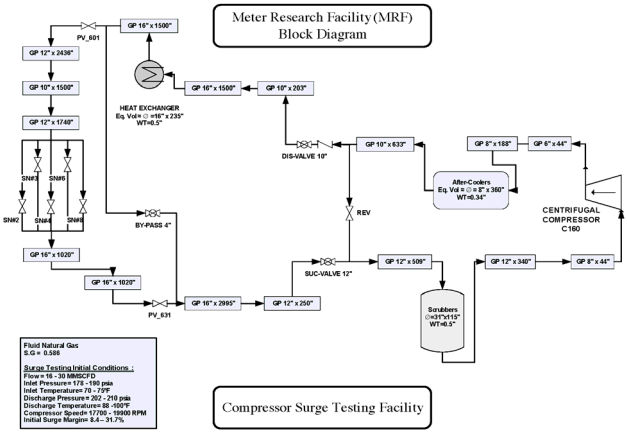

Figure 19. Meter Research Facility Block Diagram.

Model Input Data

A large amount of detailed data is required in order to develop an accurate and complete model of a centrifugal compressor and its controls. The complete piping system with lengths, diameters, and all branches or connections were defined and input into the model builder. Details such as volumes, lengths, and heat transfer surface areas were provided for coolers, heaters, scrubbers, or filters. The rotational inertia of the compressor with its driver and the torque characteristic of the driver were needed so the rate of coast down or start up could be simulated. The normal and upset condition pressures, temperatures, flows, and gas compositions were included. A complete compressor map was input for the simulation of normal and off-design operating conditions. In the MRF model, no boundary conditions were utilized, since it operates in a closed loop. All flow resistance elements were considered to ensure the modeled system impedance was as accurate as possible. Once all of the necessary data were input into the model, the program was compiled, and the model of the system was ready to simulate both steady operation and transient upsets.

Computational Model

Once a functional process block diagram was created, the computational model was developed in the TFS software. Additional detailed data specific to the equipment and piping for the process system being modeled was input into the computational model. It is important that these data be accurate in order to ensure the predictive capability of the computational model. A table of

initial operating conditions, as well as the operating constraints of the system, was generated for use in the TFS model. The model was then "tuned" so that the model accurately predicted known steady-state parameters for a specific operating point. Generally, parameters such as pipe roughness, and thermal and flow coefficients were used to adjust the model. The model was validated by comparing simulation results to known steady-state parameters at various other operating points. Comparison of the computational model versus real steady-state conditions is discussed in later sections of this paper.

Process System Simulation

Once a computational model was developed and all pertinent data were input into the model, simulations were run at various operating points. The first few operating points were used to tune and later validate the computational model. Initial steady-state (SS) conditions were simulated based on initial test conditions obtained. Initial points for the fast stop sequences were similar for experimentation and dynamic simulation. In addition, valve opening and closing sequences and the compressor coastdown speed were in concordance with the test data. All sequences were programmed in a general emergency shutdown sequence (ESD) that was initiated from each SS point for each simulated scenario. In addition, an optimum time step was determined to capture accurately the dynamic behavior of the system and its response while restricting central processing unit (CPU) time to a reasonable amount. Results of each simulation are presented in later sections of this paper.

For any system transient simulation, the following features have to be known:

- The geometry of the piping system, in particular the volumes of the piping and vessels
- The opening and closing characteristics of the valves (recycle valves, check valve)
- The inertia of the compressor train
- The thermal inertia of the driver
- The compressor performance map
- Any known delays in the surge control system

One of the key challenges in ESD simulations is to determine the correct deceleration of the train. The rate of deceleration is determined by the inertia of the train, J (referenced to compressor speed, N, for geared trains), any residual power generated by the gas turbine ($P_{GT,resid}$), the friction losses in the system, and the power absorption of the compressor.

$$P = P_{compr} + P_{frict} - P_{GT,resid} = T \cdot N = -J \cdot N \cdot \frac{dN}{dt} \tag{2}$$

$$\frac{dN}{dt} = \frac{P_{compr}(t) + P_{frict}(t) - P_{GT,resid}(t)}{-(2\pi)^2 \cdot J \cdot N(t)} \tag{3}$$

Assuming all operating points of the compressor follow the fan law, the compressor power may be expressed as:

$$P_{compr}(t) = P_o \left(\frac{N}{N_o} \right)^3 \tag{4}$$

where P_o and N_o are the steady-state power and speed at the initial operating point, respectively. Another way to determine the compressor power is to know the instantaneous operating point of the compressor (in terms of head, flow, efficiency, and suction density). But this requires a priori knowledge of the locus on the compressor map during shutdown. Assuming a constant Q/N, while not perfect, gives a reasonable assessment for the compression power. It is usually assumed that the steady-state flow-head-efficiency map of the compressor is still accurate enough to determine the consumed power at any transient operating point during the shutdown process.

Inserting Equation (4) into Equation (3) and integrating yields the following expression for the speed decay (assuming constant Q/N):

$$N(t) = \frac{J N_o^3}{J N_o^2 + P_o t} \tag{5}$$

The residual power generated by the gas turbine after the fuel valve is closed is very difficult to determine in the absence of test data. Even after the fuel valve is closed, the amount of fuel in the system, as well as the thermal inertia of the gas turbine, yields some residual power output. Moore, et al. (2009), showed the experimentally determined rate of deceleration of a different compression train. It was observed that for the first 300 milliseconds, the residual power of the gas turbine reduces the rate of deceleration. Neglecting the residual gas turbine power will lead to a more pessimistic (conservative) evaluation of the system dynamics.

Description and Considerations for MRF Model

The simulations of the model of the MRF loop were run at the measured conditions of the surge testing. The test matrices for the simulations are shown in Table 4 and Table 5. The first table is for the low energy surge events (low pressure), and the second table is for the high-energy surge events.

Table 4. Model Uncertainty Low Pressure Tests.

COMPARISON BETWEEN MODELING AND EXPERIMENTAL DATA																		
Test ID	Measured Comp Suc [psia]	Simulated Comp Suc [psia]	Comp Suc Relative Error [%]	Comp Disch [psia]	Simulated Comp Disch [psia]	Comp Disch Relative Error [%]	Tsuc [°F]	Simulated Tsuc [°F]	Tsuc Relative Error [%]	Actual Flow (cfm)	Simulated Actual Flow (cfm)	Actual Flow (cfm) Relative Error [%]	Standard Flow [MMSCFD]	Simulated Standard Flow [MMSCFD]	Standard Flow Relative Error [%]	Compressor Isentropic Head [ft]	Simulated Compress or Isentropic Head [ft]	Compress or Isentropic Head Relative Error [%]
P1-1	188.3	188.3	0.02	208.3	207.6	0.34	70.4	70.4	0.00	1400.8	1400.9	0.00	26.38	26.31	7.32	4810.0	4628.8	*3.77*
P1-2	186.2	186.2	0.01	208.1	207.6	0.24	70.7	70.7	0.03	1203.2	1203.2	0.00	22.29	24.04	7.85	5328.6	5130.4	3.72
P1-3	185.1	185.1	0.01	208.0	207.1	0.41	71.5	71.5	0.04	1071.6	1071.6	0.00	19.65	21.26	8.19	5600.7	5279.4	5.74
P1-4	184.6	184.6	0.01	207.0	207.2	0.08	72.5	72.5	0.03	938.4	938.4	0.00	17.08	18.53	8.49	5519.0	5410.3	1.97
P1-5	185.1	185.1	0.01	209.2	208.2	0.48	72.3	72.3	0.01	1618.8	1618.8	0.00	29.98	32.06	6.94	5903.4	5594.9	5.23
P1-6	182.4	182.4	0.01	209.3	208.5	0.41	73.2	73.2	0.03	1399.3	1399.3	0.00	25.34	27.28	7.66	6650.4	6315.6	5.03
P1-7	180.9	180.9	0.02	209.3	207.8	0.71	74.1	74.1	0.04	1237.6	1237.7	0.00	22.11	23.89	8.05	7044.3	6561.5	6.85
P1-8	180.6	180.6	0.02	208.3	208.1	0.12	74.8	74.8	0.01	1100.7	1100.7	0.00	19.56	21.19	8.33	6920.7	6675.4	3.54
P1-9	181.0	181.0	0.02	208.6	208.2	0.18	75.4	75.4	0.01	1101.7	1101.7	0.00	19.58	21.23	8.43	6884.3	6620.5	3.83
P1-10	180.7	180.7	0.01	202.6	202.6	0.02	73.7	73.7	0.04	941.1	941.1	0.00	16.73	18.17	8.61	5516.5	5362.7	2.79
P1-11	177.5	177.5	0.00	204.4	204.5	0.02	72.6	72.6	0.03	1072.9	1072.9	0.00	18.79	20.41	8.62	6831.6	6637.2	2.85
AVERAGE RELATIVE ERROR [%]			0.01			0.27			0.02			0.00			8.04			4.12
MODEL UNCERTAINTY[%]			1.51															

Table 5. Model Uncertainty High Pressure Tests.

COMPARISON BETWEEN MODELING AND EXPERIMENTAL DATA																		
Test ID	Compressor Speed (RPM)	Comp Suc [psia]	Simulated Comp Suc [psia]	%Error	Comp Disch [psia]	Simulated Comp Disch [psia]	%Error	Tsuc [°F]	Simulated Tsuc [°F]	%Error	Actual Flow (cfm)	Simulated Actual Flow (cfm)	%Error	Standard Flow [MMSCFD]	Simulated Standard Flow [MMSCFD]	%Error	Compressor Isentropic Head [ft]	Simulated Compressor Isentropic Head [ft]	%Error
P2-1	19804	191.7	191.6	0.04%	221.7	219.0	1.21%	71.2	71.28	0.08%	1204.0	1204.0	0.00%	23.0	22.91	0.26%	6997.3	6743.5	3.63%
P2-2	19804	195.4	195.4	0.02%	225.8	223.4	1.06%	70.3	70.37	0.04%	1195.8	1195.8	0.02%	23.3	23.26	0.13%	6942.0	6751.5	2.74%
P2-3	19805	192.0	192.1	0.05%	222.3	219.8	1.21%	70.6	70.59	0.01%	1194.6	1194.6	0.00%	22.9	22.82	0.17%	7036.2	6754.9	4.00%
P2-4	19804	195.1	195.1	0.02%	225.4	223.0	1.06%	70.6	70.57	0.01%	1202.1	1201.1	0.08%	23.4	23.33	0.21%	6637.1	6745.4	2.76%
P2-5	19806	201.3	201.3	0.00%	233.0	230.1	1.23%	71.2	71.18	0.03%	1196.9	1196.7	0.02%	24.0	23.96	0.25%	7002.1	6750.7	3.59%
P2-6	19806	201.4	201.4	0.00%	233.2	230.2	1.27%	71.1	71.09	0.06%	1199.7	1199.8	0.01%	24.1	24.04	0.19%	7036.0	6747.7	4.10%
P2-7	19802	380.2	380.2	0.01%	442.2	436.6	1.26%	67.7	67.68	0.03%	1202.8	1202.9	0.01%	47.1	46.97	0.28%	7038.3	6744.6	4.17%
P2-8	19722	380.2	380.2	0.01%	442.1	436.0	1.38%	67.7	67.70	0.03%	1203.2	1202.9	0.03%	47.1	46.96	0.38%	7040.9	6683.8	5.07%
P2-9	19722	381.3	381.3	0.01%	443.3	437.7	1.25%	68.8	68.78	0.07%	1197.8	1197.6	0.02%	46.9	46.79	0.30%	7040.5	6749.8	4.13%
P2-10	19804	377.0	377.0	0.00%	438.5	432.7	1.31%	68.4	68.43	0.01%	1201.1	1201.2	0.01%	46.6	46.49	0.37%	7052.8	6746.3	4.36%
P2-11	19804	378.3	378.3	0.01%	439.5	434.3	1.19%	68.2	68.22	0.01%	1203.7	1203.7	0.00%	46.9	46.79	0.34%	6999.0	6743.8	3.65%
P2-12	19805	379.7	379.7	0.01%	440.7	435.9	1.09%	68.2	68.21	0.03%	1204.9	1204.8	0.01%	47.1	46.92	0.34%	6950.7	6742.7	2.99%
P2-13	19803	374.9	374.8	0.03%	435.1	429.9	1.21%	68.8	68.77	0.07%	1228.5	1228.3	0.02%	46.0	47.12	2.43%	7164.3	6716.0	6.26%
Average Uncertainties				0.01%			1.21%			0.04%			0.02%			0.43%			3.99%
TOTAL MODEL UNCERTAINTY [%]				0.69%															

Simulations were run at two target speeds: 17,800 and 19,800 rpm. Flow and head conditions were set to match corresponding measured conditions and to give initial surge margins that varied from 9 to 40 percent at each speed. Based on speed data obtained during transient tests, a speed curve was used in the model to model accurately the shutdown speed transient of the compressor-gas turbine system. The models were tuned to the measured operating conditions. The error was calculated for the suction and discharge pressures and temperatures, flow, and head to access the accuracy of the model. Calculation errors for the discharge pressure were less than 1 percent for Phase 1 and less than 1.5 percent for Phase 2.

As a part of the model building process, an equivalent or hydraulic diameter for the discharge after-cooler was calculated using the wetted perimeter concept. The total area of the after-cooler was calculated by multiplying the number of tubes by the area of each tube and then the hydraulic diameter was determined utilizing Equation (6). In addition, the total volume of the cooler was calculated by adding the volume of each tube. It was found that the volume and friction factor of the cooler affect the simulation results significantly. Therefore, an initial friction factor was computed by assuming smooth pipe for the cooler and later on it was tuned using the experimental data. However, the difference between the initial assumption and the calculated friction factor using experimental data was approximately 19 percent.

$$D_h = \frac{4 * A_{tubes}}{U} = D_{tube} * \sqrt{N_{tubes}} \qquad (6)$$

where:

D_h = Hydraulic diameter
U = Wetted perimeter
D_{tube} = Tube diameter
N_{tubes} = Number of tubes

High-energy surge was simulated in the model for Phase II testing. The operating conditions of the test loop model were adjusted to have a higher discharge pressure. The recycle valve operation was varied by changing the rate at which the recycle valve opened and varying the size of the valve. This was easily done by varying different parameters of the recycle valve model. As discussed previously, recycle valve travel times varied from 100 to 300 percent of normal operation when the valve was fully opened during shutdown (normal operation was 1.81 seconds) and the flow restriction or size of the valve was varied from 5 to 100 percent of normal operation. All the tests were completed at an initial speed of 19,800 rpm. The operating conditions were set in the model such that each test was started with an initial surge margin of 20 percent. The error was calculated for the high surge simulations based on the difference between measured and simulated parameters.

MODELING RESULTS

Compressor speed decay curves and valve opening and closing sequences were either calculated or obtained from manufacturers' datasheets. These assumed values were compared to prediction, and the model was systematically improved. All those sequences were programmed in a general emergency shutdown sequence that was initiated from each steady-state point for each simulated scenario. In addition, an optimum time step was determined to capture accurately the dynamic behavior of the system and its response. Results of each simulation were presented in a chart of head versus actual flow including the compressor performance map for further comparison with the test data. Moore, et al. (2009), compare the measured and predicted speed decay using Equation (5). The measured speed decay was slightly faster than the prediction. Due to the relatively low suction pressure and aerodynamic power for this compressor, other losses from bearings (which were accounted for) and power turbine losses were a high percentage of the total power compared to a typical pipeline compressor installation. Therefore, the difference between the measured and predicted speed curves is expected to be less for most applications.

Figure 20 is an example of the valve sequence timing used for simulation. The example shown is for a calculated rpm decay curve. As the recycle valve was fully characterized before testing, the opening time and open CV was tailored for each simulation to match the corresponding experiment. Figure 20 shows the measured quasi-linear rpm decay behavior discussed earlier in contrast to the calculated rpm decay curve.

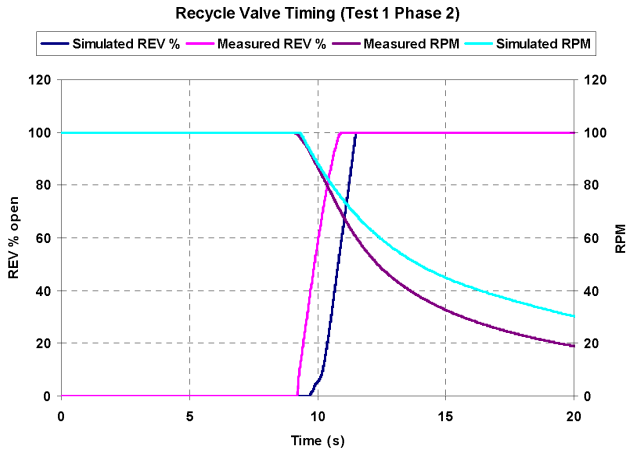

Figure 20. Shutdown Sequence Timing Using a Calculated RPM Decay for the Simulation for Test 1 of Phase II.

Phase 1 Test Conditions

Figure 21 through Figure 23 report the results of both the simulated and measured (experimental) tests. For all cases, there was good agreement, with some over-prediction of the flow minimum in the simulated tests. When designing anti-surge systems, conservative design factors are always used. An over-prediction of minimum flow will serve to strengthen this safety factor. Even tests with low initial surge margins were well predicted by TFS, as seen in P1- 7, 8, and 11 (Figure 23).

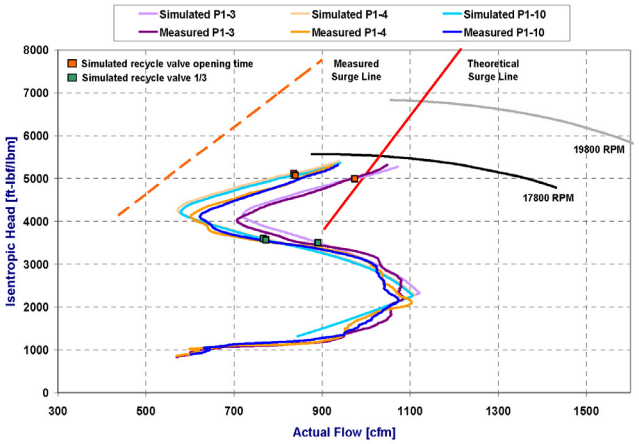

Figure 21. Compressor Map with Measured and Simulated Transient Events from 17,800 RPM (A).

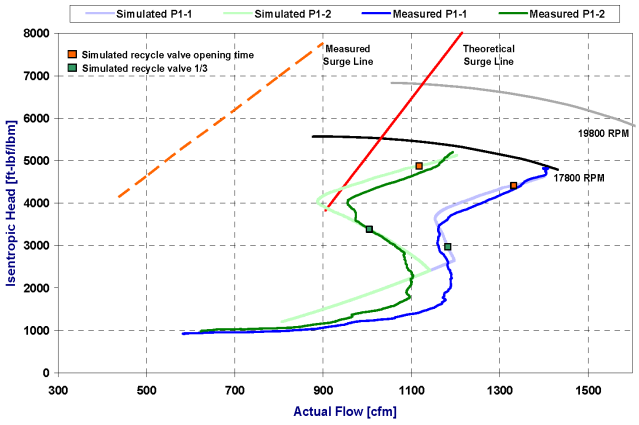

Figure 22. Compressor Map with Measured and Simulated Transient Events from 17,800 RPM (B).

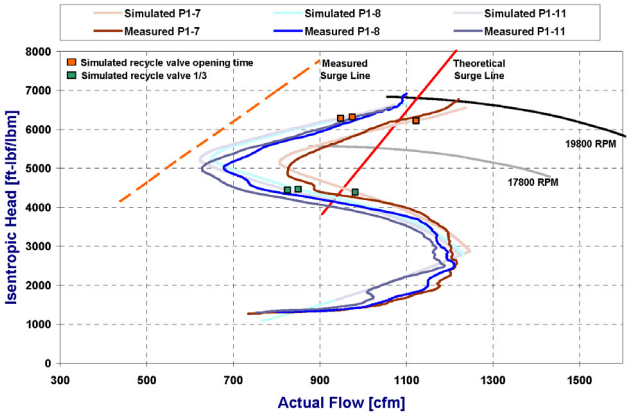

Figure 23. Compressor Map with Measured and Simulated Transient Events from 19,800 RPM.

From the simulated and measured results, it is clear that the theoretical surge line did not predict surge well. No surge cycles (i.e., rapidly increasing and decreasing flow rates with a gradual drop in head) or erratic loci were observed in the measured data for low suction pressure testing (Phase I). Moore, et al. (2009), provide additional comparisons for the Phase I results.

Phase II Test Conditions

Figure 24 through Figure 27 contain a comparison of simulated and measured data for Phase II testing. Similar to what was observed in Phase I, there were significant differences between simulations using an rpm decay curve that was calculated versus a measured curve from Phase II experimentation. Simulations using the calculated curve produced better results than the simulations using the measured curve. The simulated results contained in the following graphs were generated using the calculated rpm decay curve.

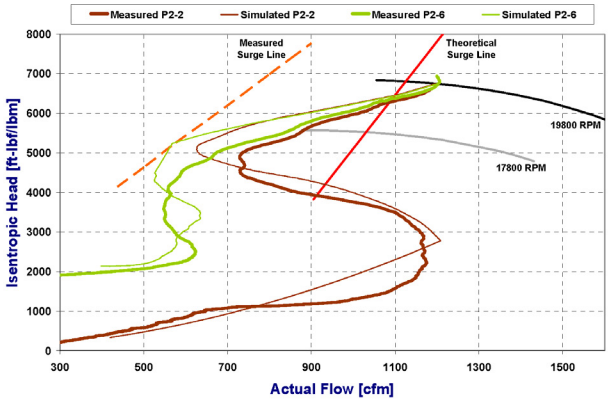

Figure 24. Simulated and Measured Data Comparison (Phase II)—A.

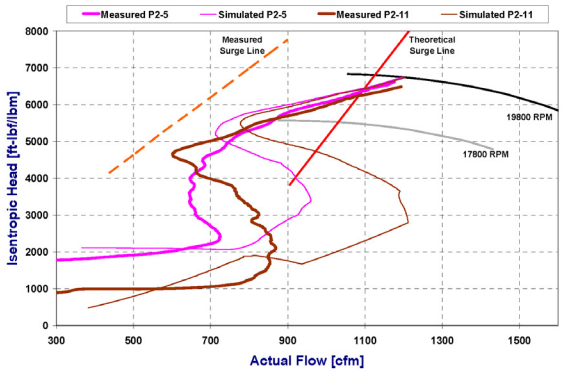

Figure 25. Simulated and Measured Data Comparison (Phase II)—B.

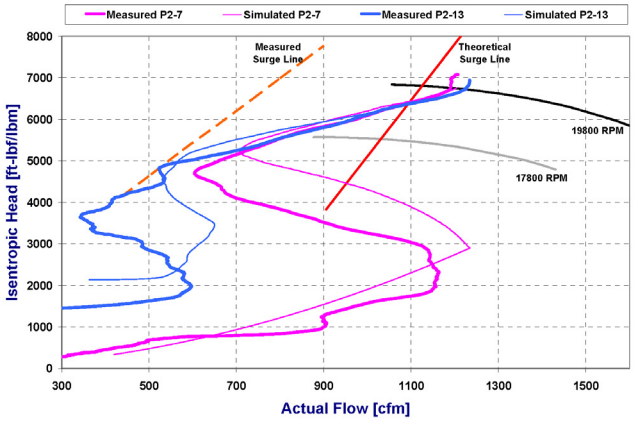

Figure 26. Simulated and Measured Data Comparison (Phase II)—C.

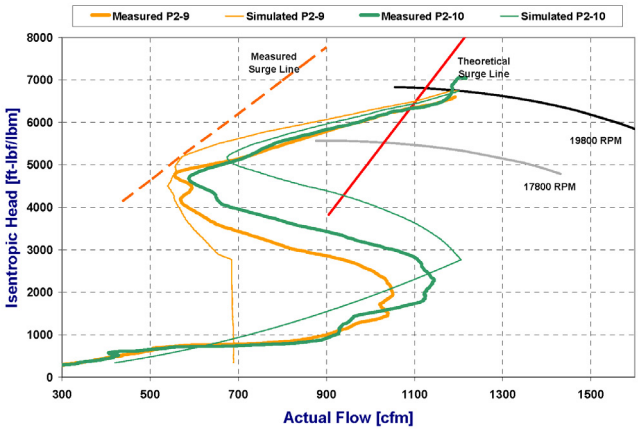

Figure 27. Simulated and Measured Data Comparison (Phase II)—D.

ANALYSIS OF RESULTS

Phase I testing using lower suction pressure demonstrated good agreement between simulation and measured data. Minimum flow and loci trends were well predicted and matched closely when compared to Phase II testing. At stonewall and surge conditions, the model was unable to predict trends as TFS does not extrapolate compressor maps. In addition, because meaningful compressor performance data in this region are unknown, extrapolation may not be a valid method of extending the map. Data were given only for the envelope bounded on the left by the measured surge line and on the right by stonewall (choked) conditions. Loci that showed signs of trending outside this envelope ended up following the surge or stonewall line (e.g., Figure 23). Predicting trends at the stonewall condition may not be of importance, as the compressor is in little to no danger of surging while coasting down in this region. Predicting trends at the surge line is of more importance as the severity and duration of the surge cannot be accurately predicted. Test P2-13 (Figure 26) was the only test that showed clear signs of a significant surge event. The simulation accurately predicted the entry point to the surge but did not give any meaningful data after that point. The measured data showed an increase in flow shortly after surge started; however, no flow increase was shown in the simulation.

Phase II simulations did not correlate as well to experimental data when compared to Phase I results. Whereas loci trends were fairly well conserved through compressor deceleration for the simulated results of Phase I (as compared to the measured data), simulated results from Phase II often did not trend as well. A good example is found in Figure 25. Minimum flow was not well predicted using either calculated or measured rpm decay curves; significant under- and over-prediction was observed. There were cases where this mismatch in minimum flow prediction could have detrimental effects on anti-surge system design. Test P2-7, shown in Figure 26,

showed a severe under-prediction of minimum flow. Simulations may have shown adequate protection for the compressor; however, the measured data showed a dangerously low minimum flow condition that was quite close to the measured surge line. Good agreement between simulated and measured data was shown for most cases before the minimum flow condition was reached; however, TFS did not appear to predict surge or near-surge conditions well. If the minimum flow condition occurred near the measured surge line, simulated and measured data diverged considerably after this point was transitioned. Where some measured tests show rapidly increasing and decreasing flow with an associated drop in head, corresponding simulated tests either drastically increased flow or damped out (smoothed) the details of the loci. This damping of detailed effects near surge appeared to affect simulations as rpm decay continued, evident by the continued mismatch of loci after the minimum flow point. It should be noted that the compressor curves to the left of the theoretical surge line were not well known and were likely the cause of some of the error for these cases.

A significant result from this study was the impact that speed decay modeling had on the accuracy of the solution. As shown in Moore, et al. (2009), calculated speed decay was slower than measured decay. Of particular importance were the first two seconds of decay, when a potential surge event was likely to occur. During this period, the measured and calculated decay curves differed by 0 to 8 percent of total rpm. This difference produced surprisingly different results. Figure 28 is a reproduction of Figure 26, with simulation results using measured speed decay curves added. This figure lends an appreciation to the accuracy required in modeling speed decay. Using the test cases in Figure 28 as an example, a 5 percent erroneous reduction in rpm at the initial point of 19,800 rpm translated to a 9.4 percent error in head. Such an error has significant impact on surge prediction and loci trends. At this point, it is unclear as to why the calculated speed decay curve gave better results, as the solution method used by TFS was a black box and not open to analysis.

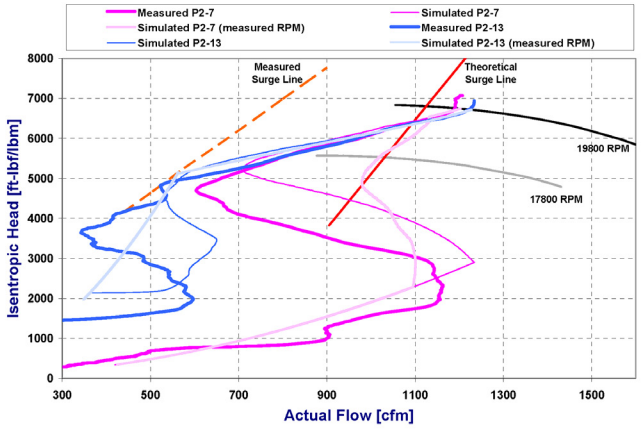

Figure 28. Comparison of Measured and Calculated RPM Decay Curves on Simulation Results.

CONCLUSIONS AND COMMENTS

A highly accurate series of surge test data has been gathered and compared to a state-of-the-art transient simulation. For certain conditions, the code accurately predicted the transient shutdown behavior of a centrifugal compression station without specific tuning of the model. The data quality and detail allowed using the transient software without the uncertainties usually involved in modeling a new compression system.

The analysis did under-predict the speed decay rate during shutdown, and the predictions generally got worse using the measured rather than predicted speed decay. Some of this difference was likely due to the simple assumptions (fan law) made in the derivation. Transient codes usually require some assumption about the rate of speed decrease, and this can be a major source of inaccuracy. The analytical model accuracy could also be improved if steady-state test data are gathered in order to refine the pressure drops and pipe friction factors throughout the domain. Further refinement could be achieved if actual valve opening times in the installed operating condition could be obtained.

Good agreement was obtained between measured and simulated cases for low suction pressure testing without recycle valve modification. Poorer agreement was observed for higher suction pressures and for tests that modified the recycle valve characteristics. TFS did not predict test cases well that passed through a region close to the measured surge line or crossed it. These tests often involved rapidly changing flow rates, which were damped out in the corresponding simulation. Further tests are recommended to evaluate conclusively how effective TFS is at predicting rapidly changing flow characteristics, as are often present during surge or near-surge transient events. Practically speaking, well-designed surge control systems should not cross the actual surge line, which would improve the predictions.

Successful modification of recycle valve characteristics resulted in equivalent valve sizes of 1.2 inches to full scale (6 inches) with a variety of travel times. The anti-surge system was thus modified to permit testing near the surge line, including one test that entered full surge. It was found that the recycle valve was significantly over-designed for the conditions tested.

Simulated results were sensitive to the rpm decay data used. A small difference in rpm during the first few seconds of the shutdown event produced drastically different results. An rpm decay curve was calculated, and a second rpm decay curve, based upon actual rpm decay data from the experiment, was also used. Contrary to expectations, the actual rpm decay curve produced worse results than the calculated curve. The cause of this unexpected result could be a subject for further investigation.

NOMENCLATURE

Cv	= Valve flow coefficient (gpm/psi^{½})
H	= Head (ft-lbf/lbm)
J	= Inertia (lbm-in^2)
N	= Speed (rpm)
NPT	= Power turbine speed (rpm)
P	= Power (hp)
p	= Pressure (psi)
Q	= Flow (ACFM)
T	= Compressor torque (ft-lbf)
W	= Mass flow (lbm/s)
ω	= Rotational speed (rad/sec)

ABBREVIATIONS

ASV	= Anti-surge valve
ESD	= Emergency shutdown
GT	= Gas turbine
MRF	= Metering research facility

REFERENCES

Botros, K. K. and Ganesan, S. T., 2008, "Dynamic Instabilities in Industrial Compression Systems with Centrifugal Compressors," *Proceedings of the Thirty-Seventh Turbomachinery Symposium*, Turbomachinery Laboratory, Texas A&M University, College Station, Texas, pp. 119-132.

Brun, K. and Nored, M., 2007, "Application Guideline for Centrifugal Compressor Surge Control Systems," Gas Machinery Research Council.

Kurz, R. and White, R. C., 2004, "Surge Avoidance in Gas Compression Systems," ASME Journal of Turbomachinery, *126*, (4).

Moore, J. J., Garcia, A., Blieske, M., and Brun, K., 2008, "Full Scale Testing of Centrifugal Compressor Surge to Develop Benchmark Data for Transient Analysis Software," GMRC Report, http://www.gmrc.org/projects-2004.html

Moore, J. J., Kurz, R., Garcia, A., and Brun, K., 2009, "Experimental Evaluation of the Transient Behavior of a Compressor Station During Emergency Shutdowns," ASME GT2009-59064, Proceedings of ASME Turbo Expo 2009: Power for Land, Sea, and Air.

Morini, M., Pinelli, M., and Venturini, M., 2007, "Application of a One-Dimensional Modular Dynamic Model for Compressor Surge Avoidance," Proceedings of ASME Turbo Expo 2007: Power for Land, Sea, and Air.

Ribi, B. and Gyarmathy, G., 1997, "Energy Input of a Centrifugal Stage into the Attached Piping System During Mild Surge," ASME 97-GT-84.

White, R. C. and Kurz, R., 2006, "Surge Avoidance for Compressor Systems," *Proceedings of the Thirty-Fifth Turbomachinery Symposium*, Turbomachinery Laboratory, Texas A&M University, College Station, Texas, pp. 123-134.

ACKNOWLEDGEMENTS

The authors would like to thank the Gas Machinery Research Council, ExxonMobil, Solar Turbines, and BP for funding this work.